Journal of Dental Sciences 19 (2024) 2114–2125

Available online at www.sciencedirect.com

ScienceDirect

journal homepage: www.e-jds.com

Original Article

Enhanced bone formation of rat mandibular bone defects with collagen membranes loaded on bone morphogenetic protein-9

Hiroki Kondo [a†], Tadahiro Takayama [b,c*†], Takashi Onizawa [a], Shunsuke Isobe [a], Natsuko Tanabe [d,e], Naoto Suzuki [d,e], Seiichi Yamano [f], Shuichi Sato [b,c]

[a] *Division of Applied Oral Sciences, Nihon University Graduate School of Dentistry, Tokyo, Japan*
[b] *Department of Periodontology, Nihon University School of Dentistry, Tokyo, Japan*
[c] *Division of Advanced Dental Treatment, Dental Research Center, Nihon University School of Dentistry, Tokyo, Japan*
[d] *Department of Biochemistry, Nihon University School of Dentistry, Tokyo, Japan*
[e] *Division of Functional Morphology, Dental Research Center, Nihon University School of Dentistry, Tokyo, Japan*
[f] *Department of Prosthodontics, New York University College of Dentistry, NY, USA*

Received 4 March 2024; Final revision received 4 April 2024
Available online 17 April 2024

KEYWORDS
Bone morphogenetic protein-9;
Bone regeneration;
Collagen membrane;
Rat mandibular bone defects;
Real-time in vivo micro-computerized tomography

Abstract *Background/purpose:* Bone morphogenetic protein-9 (BMP-9) has demonstrated multiple advantages in promoting osteogenesis. Our previous findings have indicated that the use of an absorbable collagen membrane (ACM) as a carrier for growth factors is effective in stimulating bone regeneration. The objective of this study was to assess the synergistic impact of BMP-9 incorporated into ACM (ACM/BMP-9) on bone formation within rat mandibular bone defects.

Materials and methods: Circular bone defects of critical size were surgically induced on both sides of the rat mandibular bone, with subsequent random allocation into distinct groups: control, ACM alone, and ACM loaded with low (0.5 μg) or high (2.0 μg) concentrations of BMP-9. We conducted real-time in vivo micro-computerized tomography scans at the baseline and at 2, 4, and 6 weeks, and measured the volume of newly formed bone (NFB), bone mineral density (BMD) of NFB, and the closure percentage of the NFB area. Histological and histomorphometric analyses were performed at 6 weeks.

Results: Real-time assessment revealed notably higher levels of bone volume, BMD, and closure percentage in the NFB area for the groups treated with ACM/BMP-9 compared to the

* Corresponding author. Department of Periodontology, Nihon University School of Dentistry, 1-8-13 Kanda-Surugadai, Chiyoda-ku, Tokyo 101-8310, Japan.
E-mail address: takayama.tadahiro@nihon-u.ac.jp (T. Takayama).
† These authors contributed equally to this work.

https://doi.org/10.1016/j.jds.2024.04.004

control and ACM groups. Within the high concentration of BMP-9 group, the volume and BMD of NFB exhibited a significant increase at 6 weeks compared to baseline. Histological examination confirmed the existence of osteoblasts, osteocytes, and blood vessels within the NFB.
Conclusion: Considering the limitations of this research, the real-time evaluation finding indicates that ACM/BMP-9 effectively promotes bone formation in critical-size mandibular defects in rats.

Introduction

Insufficient bone volume at the implant site may cause notable clinical complications and needs to be augmented before the placement of the implant.[1] To attain effective bone tissue repair, clinicians frequently employ guided bone regeneration (GBR).[2] This technique is extensively utilized in dental implant procedures to enhance the available bone for supporting the implant. Additionally, GBR can manage bone deficiencies resulting from periodontal disease or traumatic injuries. GBR is a surgical procedure designed to promote the growth of new bone tissue in areas where bone loss has occurred due to trauma or periodontal disease.[3]

The barrier membrane serves as a protective barrier, inhibiting the infiltration of soft tissue like fibroblasts, while facilitating the migration of bone cells into the site and form new bone. The objective is to block and prevent the rapid movement of epithelial cells and fibroblasts toward the defect site by inserting a membrane between the hard tissue and the soft tissue.[4] Five primary criteria have been established to delineate favorable attributes of the membrane employed in GBR therapy. These criteria encompass biocompatibility, occlusive properties, ease of clinical handling, space maintenance, and possessing sufficient mechanical properties.[5] Biodegradable barrier membranes derived from natural sources, like collagen, chitosan, gelatin, silk, are crafted for medical applications. These materials are intentionally designed to be absorbed naturally within the patient's body over time, promoting the gradual replacement of the implanted membrane with the patient's own tissue during the recovery period.[6]

Collagen has become a focal point in GBR applications. Biologically, it plays a vital role in the extracellular matrix, serving as a structural scaffold that facilitates cell attachment and proliferation. In GBR applications, collagen has the capability to stimulate cell adhesion and growth, improving tissue regeneration and the bone formation. Moreover, collagen can serve as a carrier for diverse bioactive substances like growth factors, intensifying the process of bone regeneration.[7] In terms of material attributes, collagen exhibits favorable qualities for GBR, including biocompatibility, biodegradability, and minimal immunogenicity.[8] Collagen-based carriers are increasingly prevalent in clinical and translational research.[9,10] Nevertheless, to achieve optimal clinical results, modifications are necessary for this material. These adjustments aim to enhance healing speed and ensure a higher quantity and quality of the regenerated bone. Hence, the latest advancements incorporate the utilization of membranes created through tissue engineering, a concept previously introduced by Sam and Pillai.[11] These advanced membranes not only function as barriers but also have the capability to release specific agents, such as antibiotics, growth factors, and adhesion factors, in a controlled manner at the site of the wound. This approach aims to enhance and regulate the natural wound healing process more efficiently. Indeed, in this generation, there is a synergistic use of resorbable membranes and growth factors to accelerate cell migration, proliferation, differentiation, and the deposition of extracellular matrix. This synergy results in quicker and more effective tissue regeneration.[12,13] Additionally, this approach allows for a controlled release of growth factors, reducing the necessary dosage and minimizing potential side effects. These growth factors can be integrated into the membrane matrix during manufacturing or applied to the membrane surface post-fabrication.[14] The application of absorbable collagen membranes (ACMs) with incorporated growth factors around bone defects contributes to enhanced healing of osseous defects in GBR sites.

In this context, we offer a thorough examination that specifically concentrates on assessing the effectiveness of collagen barrier membranes coupled with growth factors. These growth factors encompass growth/differentiation factor 5, stromal cell-derived factor-1, osteogenic protein-1, and fibroblast growth factor-2, of our previous studies.[15–18] We've introduced novel applications employing ACMs containing growth factors with dual functions: preventing the migration of soft tissue growth to maintain space for bone and enhancing the healing of bone. This effort aims to further improve clinical outcomes, encompassing the healing phase, quality, and quantity of newly formed bone. Additionally, we have explored new potential growth factors to enhance the efficacy of bone regeneration.

Through adenovirus transfection experiments comparing various bone morphogenetic proteins (BMPs), it was found that BMP-9 exhibits superior osteogenic potential compared to clinically approved BMP-2 and BMP-7.[19] Intriguingly, rhBMP-9 combined with an absorbable collagen sponge (ACS) demonstrated greater osteogenic potential than surgical control or ACS alone. This combination also resulted in new bone formation with reduced adipose tissues compared to rhBMP-2/ACS in rat critical-

sized calvaria bone defects.[20] Additionally, recent in vitro research indicated that rhBMP-9 can enhance osteoblast differentiation, leading to increased alkaline phosphatase production and alizarin red staining even at doses 20 times lower than rhBMP-2 and rhBMP-7.[21] Consequently, rhBMP-9 might serve as an effective alternative to rhBMP-2, inducing bone formation at lower doses and potentially reducing secondary side effects and treatment costs.[22]

In our pursuit of enhanced clinical outcomes and the identification of novel growth factors for effective bone regeneration, we devised a novel regenerative unit that integrates an absorbable collagen membrane containing BMP-9 (ACM/BMP-9) for bone regeneration. However, there is a lack of data regarding the application of ACM/BMP-9 for critically-sized circular bone defects in vivo. Additionally, the accurate real-time assessment of physical parameters, such as the volume and mineral density of newly formed bone (NFB) at specific intervals, offers comprehensive insights into bone dynamics and the duration required for osseous healing in bone defects. Remarkably, there are no documented studies on real-time variations in NFB volumes and mineral densities utilizing ACM/BMP-9 in standardized mandibular defect treatments within live animal models. Consequently, the present study aimed to explore the efficacy of ACM/BMP-9 on promoting bone regeneration in rat mandibular bone defects through real-time in vivo micro-computed tomography (micro-CT) and conventional histological evaluation.

Material and methods

Preparation of absorbable collagen membranes containing bone morphogenetic protein-9

A commercially available ACM (BioMend®; Hakuho, Tokyo, Japan) consisting of cross-linked bovine type I collagen was utilized for in vitro (size: 5 mm × 7.5 mm) and in vivo (size: 5 mm × 15 mm) studies. Prior to initiating the experiment, the ACMs were loaded with a carrier-free recombinant rat BMP-9 solution (R&D Systems, Minneapolis, MN, USA) at low (0.5 μg, L) or high (2.0 μg, H) concentration.

Release kinetics of bone morphogenetic protein-9 from the absorbable collagen membranes using enzyme-linked immunosorbent assay (ELISA)

The release kinetics of BMP-9 from ACMs were assessed in vitro at 37 °C within 2 ml of phosphate-buffered saline (PBS, pH 7.2; Fujifilm Wako Co., Osaka, Japan) over a duration of 2 weeks. At scheduled intervals, 2 ml of PBS containing FGF-2 was extracted and replaced with an equal volume of fresh PBS on days 2, 4, 6, 10, and 14. Samples were preserved at −20 °C until the time of testing. All collected samples were underwent centrifugation and filtration to eliminate free-floating impurities before being quantitatively analyzed using a rat BMP-9 ELISA kit (R&D Systems, Minneapolis, MN, USA) at the end of the experiment. The presented data represent findings from a singular experiment (n = 3) replicated twice.

Study animals

This study utilized ten male Fischer 344jcl rats at 10 weeks of age, each weighing 250 ± 20 g. The rats were acclimated to the laboratory conditions for 7 days at a temperature of 23−24 °C, humidity of 55%, and 12-h dark−light cycles. Housed in pairs in a specific pathogen-free environment, the rats had access to standard commercial food and tap water *ad libitum*. The research protocol received approval from the local animal ethics committee in accordance with the Guidelines for Animal Experiments of Nihon University (AP19DEN013-2, AP22DEN022-1).

Surgical protocol

Prior to surgery, the rats were lightly anesthetized by inhaling isoflurane with O2 and subsequently underwent deep anesthesia through intraperitoneal (i.p.) administration of a mixture comprising 0.15 mg/kg dexmedetomidine hydrochloride (Fujifilm Wako Co., Osaka, Japan), 2.0 mg/kg midazolam (Astellas Pharma Inc., Tokyo, Japan), and 2.5 mg/kg butorphanol tartrate (Meiji Seika Pharma Co., Tokyo, Japan). The anesthetic doses were precisely adjusted according to the animal's weight to minimize potential adverse reactions associated with general anesthesia. To control bleeding and enhance anesthesia, an intraperitoneal injection of 500 μl of a 1:80,000 dilution of lidocaine (Xylocaine; Astra Zeneca, Osaka, Japan) was administered. The surgical area was shaved and cleaned with 70% ethanol (Fujifilm Wako Co., Osaka, Japan) before surgical incision.

A sterile No. 15 surgical blade (Feather Co., Osaka, Japan) was utilized to make an incision in the skin. The incision extended through the entire thickness of the muscle around the mandibular angle and the underlying periosteum. Subsequently, the skin and periosteum were excised to expose the mandibular bone. After identifying anatomical landmarks, experimental mandibular bone defects were created on both sides using a 4.0 mm diameter bone trephine bur (Dentech, Tokyo, Japan) mounted on a rotary handpiece and irrigated with 0.9% saline solution (Fujifilm Wako Co., Osaka, Japan).

In the groups treated with a membrane, we applied a barrier membrane to cover the defect on both the buccal and lingual sides (Fig. 1). Following the surgical procedure, the muscle and skin layers were repositioned and sutured closed using 5-0 resorbable sutures (Alfresa Pharma Co., Osaka, Japan). All animals were monitored until they recovered from anesthesia, at which point they were returned to their cages. A soft commercial diet was provided for the first 7 days postoperatively, followed by a regular diet until euthanization.

The mandibular defects in the rats were randomly allocated to one of four experimental groups, each consisting of 5 rats: (1) control group, receiving no treatment; (2) ACM group, where the defect was covered with ACM alone; (3) L-BMP-9 group, involving the coverage of the defect with ACM containing 0.5 μg BMP-9; and (4) H-BMP-9 group, where the defect was covered with ACM containing 2.0 μg BMP-9.

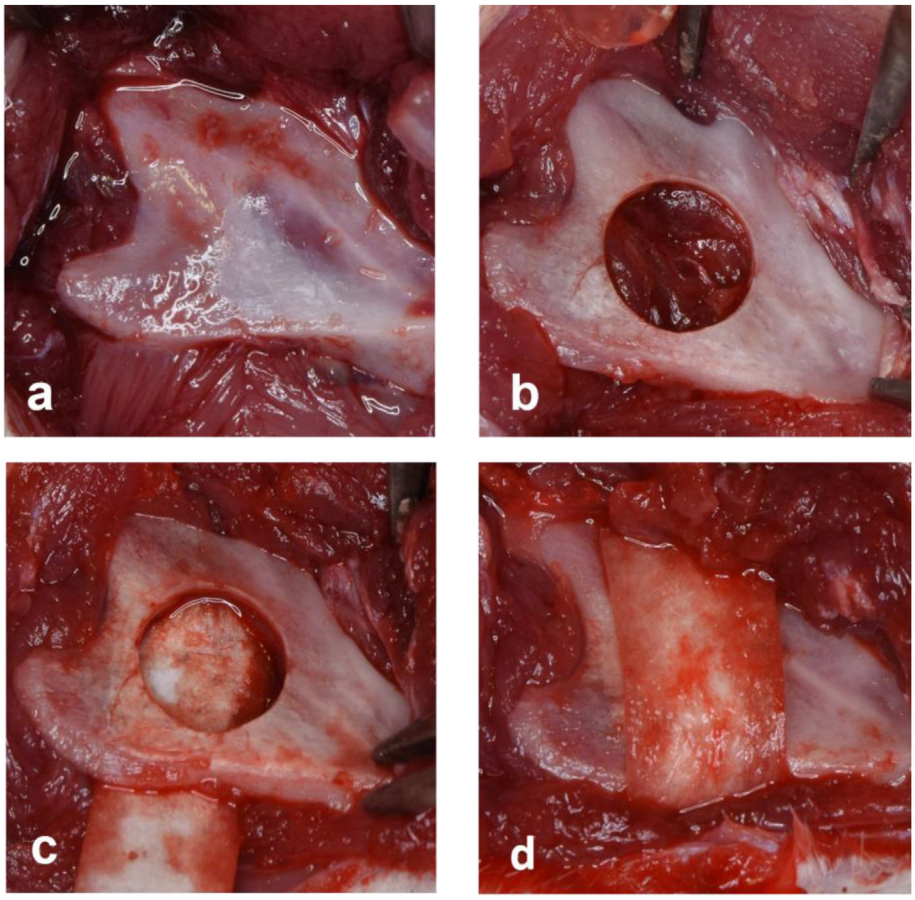

Figure 1 Surgical protocol. (a) After making an incision on the mandibular ramus, we created a full-thickness flap and reflection to expose the mandibular angle site. (b) An experimental defect of 4 mm diameter was created by using a trephine drill on the right side of the mandible ramus. (c) Placement of an inner resorbable collagen membrane between the mandibular bone and the underlying periosteum. (d) Placement of a resorbable collagen membrane completely over the circular bone defect at the mandibular angle.

Real-time in vivo micro-computed tomography evaluation

The micro-CT scanning protocol comprised an initial scan conducted immediately after surgery, followed by subsequent scans at 2, 4, and 6 weeks postoperatively. Three-dimensional (3D) isosurface rendering and image construction were carried out using i-View software (Kitasenjyu Radist Dental Clinic; i-View Image Center, Tokyo, Japan) in accordance with the manufacturer's guidelines. Representative sections were extracted from the vertical view after 3D reconstruction. Microstructural properties of bone were quantified using the standard resolution mode. The R_mCT2 system (Rigaku, Tokyo, Japan) was employed for micro-CT assessment of new bone formation within the defect region. The CT settings were as follows: pixel matrix, 480 $\times$ 480; voxel size, 30 $\times$ 30 $\times$ 30 μm; slice thickness, 120 μm; tube voltage, 90 kV; tube current, 100 μA; and exposure time, 17 s. The region of interest was selected around the newly formed bone (NFB), and the bone volume (BV) and bone mineral density (BMD) of the NFB within the circular defects were automatically acquired and measured from voxel images using BV-measurement software (Kitasenjyu Radist Dental Clinic; i-View Image Center, Tokyo, Japan). The volumes of new bone formation (NBV) were measured in cubic millimeters (mm^3), and their BMD was measured in grams per cubic millimeter (mg/cm^3). Micro-CT imaging was conducted regularly from the baseline to 6 weeks after surgery.

Histological analysis

At the conclusion of the 6-week observation period following the defect operation, all animals were humanely euthanized using carbon dioxide. The mandibular ramus was removed and preserved in a 10% neutral-buffered formalin solution (Fujifilm Wako Co., Osaka, Japan). After 14 days of fixation, histopathological examination was conducted on all mandibular defect sites. The samples were dissected and subjected to a 5-day decalcification process in K-CX (Falma, Tokyo, Japan). Following decalcification, the samples were dehydrated with graded ethanol, defatted in xylene (Fujifilm Wako Co., Osaka, Japan), and embedded in paraffin. Microtome cutting produced 5-μm sections of the embedded tissues. These sections were stained with hematoxylin and eosin for

histological assessment. Image capture was performed using a polarizing microscope (Eclipse LV100POL; Nikon Instech Co., Ltd., Tokyo, Japan), and the histology sections were examined at the Department of Pathology, Nihon University School of Dentistry.

Histomorphometric analysis

The assessment of NFB within the defects in each group involved the use of micro-CT images and histological sections. In micro-CT analysis, the measurement of new bone areas was accomplished by quantifying the number of pixels representing hard tissues within the boundaries of the NFB. Additionally, the defect closure rate, determined by measuring the area within the circular bone defect edges, was expressed as a percentage of the square of the overall defect. The new bone ratio in each of the measured areas described above was quantified using ImageJ software (National Institutes of Health, Bethesda, MD, USA).

Statistical analysis

Each value is expressed as the mean ± standard error (S.E.M). To assess differences in NBV, BMD, and the defect closure rate within and between groups, a two-way analysis of variance (ANOVA) was employed. A significance level of 0.05 was set for all statistical comparisons. Post-hoc analysis using Tukey's method was conducted to identify pairs of groups exhibiting statistical differences. Statistical analyses were carried out using GraphPad Prism 5 software (GraphPad Inc., La Jolla, CA, USA), with *P* values below 0.05 considered significant for all analyses.

Results

In vitro release profile of bone morphogenetic protein-9 from absorbable collagen membranes

Fig. 2 shows the kinetic release of BMP-9 in vitro. In this experiment, a combined device was prepared by adding 0.5 μg or 2.0 μg of BMP-9 to ACM. ACM containing BMP-9 exhibited a sustained release profile for the two different effective doses (0.5 or 2.0 μg) during the 1- to 14-day period. The cumulative release of BMP-9 from ACM reached approximately 100% within 6 days, followed by a gradual decrease.

In vivo effect of absorbable collagen membranes/bone morphogenetic protein-9 on bone regeneration

Representative images from the micro-CT scan of the mandibular defects in rats from baseline to 6 weeks are shown in Fig. 3A. Based on the structural morphology of the defects, we inferred that the isolated islands of particulates in the defects were NFB. Examination of the ACM/BMP-9 groups indicated that bone formation in the BMP-9-treated defects was higher than that in the control or ACM groups. However, the NFB in the H-BMP-9 group was higher than that in the L-BMP-9 group. Moreover, new bone filled the defects at 6 weeks after surgery in the H-BMP-9 group. These observations are consistent with the quantitative results shown in Figs. 3B and 4.

The micro-CT analysis results revealed an increase in NBV within the mandibular defects throughout the study period in all groups (Figs. 3B and 4 and Table 1). At 6 weeks, the highest NBV was observed in the H-BMP-9 group (19.93 ± 2.66 mm^3), followed by the L-FGF-2 (17.75 ± 5.34 mm^3), RCM alone (9.37 ± 2.01 mm^3), and control groups (8.10 ± 1.55 mm^3). The NBV in the BMP-9-treated groups was significantly higher than that in the control group throughout the study, with higher bone formation in the H-BMP-9 group than that in the L-BMP-9 group (Fig. 4). In addition, there was a significant increase in the NBV from baseline at 6 weeks in the H-BMP-9 groups ($P < 0.01$), and as early as 2 weeks in the BMP-9 treated groups ($P < 0.05$). During weeks 2 and 4, the NBVs in the BMP-9-treated groups were significantly higher than those in the control and RCM groups ($P < 0.05$). The highest increase in NBV occurred within the first 2 weeks in all the test groups. Table 2 illustrates the rate of increase in NBVs. The BMD of the NFB increased from baseline to 6 weeks in both the control and test groups (Figs. 3B and 4 and Table 1). At 6 weeks, the H-BMP-9 group had the highest BMD (400.53 ± 62.49 mg/mm^3), followed by L-BMP-9 (303.53 ± 96.53 mg/mm^3), RCM (257.53 ± 8.79 mg/mm^3), and control groups (102.53 ± 1.08 mg/mm^3). We observed

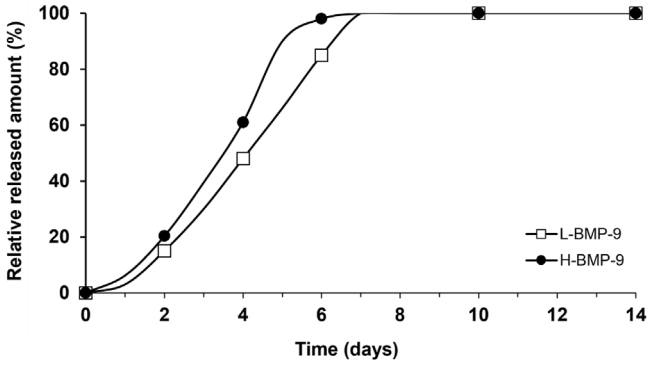

Figure 2 Recombinant rat bone morphogenetic protein (BMP)-9 release profile of the absorbable collagen membrane (ACM) containing BMP-9.

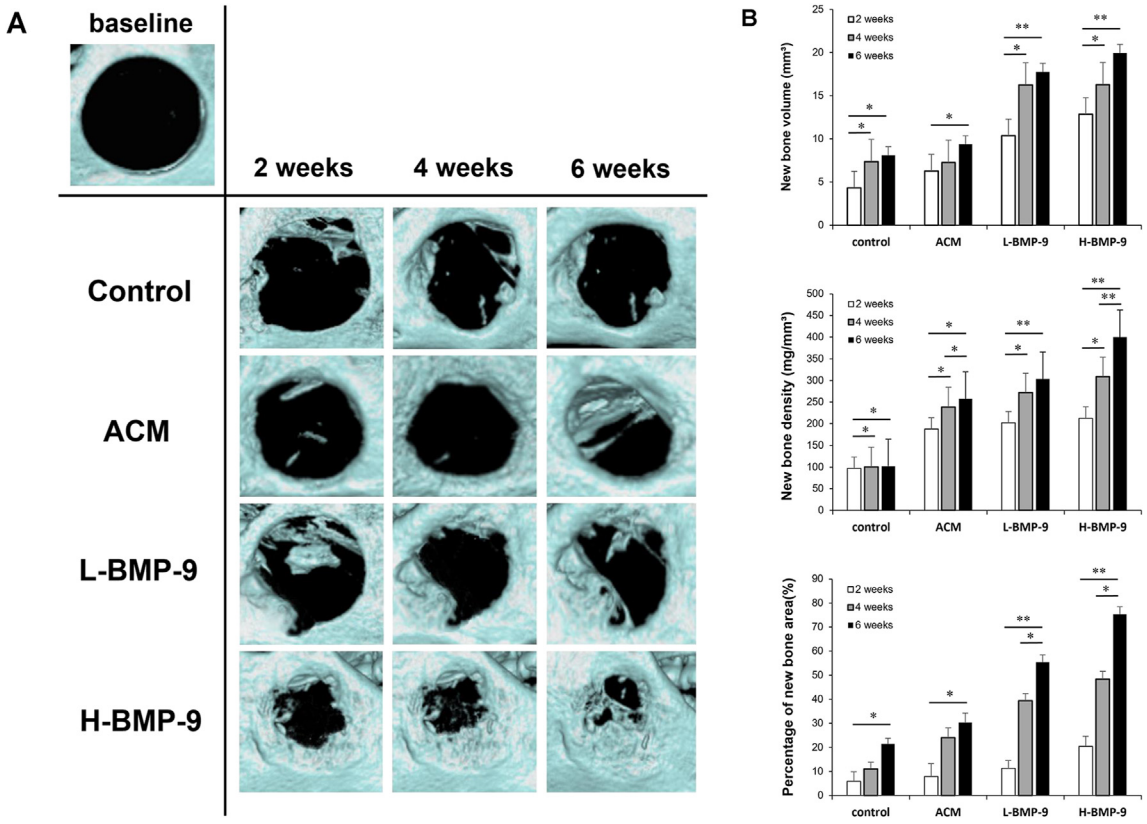

Figure 3 (A) A series of reconstructed in vivo real-time micro-CT representative images of new bone formation in rat mandibular defects at baseline, 2, 4, and 6 weeks after surgical procedures in four groups: control, absorbable collagen membrane (ACM) alone, ACM containing a low dose of 0.5 μg of bone morphogenetic protein (BMP)-9 (L-BMP-9), and ACM containing a high dose of 2.0 μg of BMP-9 (H-BMP-9). The black color shows non-mineralized defects. (B) The quantitative micro-CT analysis of new bone formation, (a) bone volume (mm^3), (b) new bone density (mg/cm^3), and (c) the percentage of new bone area (%) in rat mandible defects treated with absorbable collagen membrane (ACM)/bone morphogenetic protein (BMP)-9 throughout the experimental period. Four groups were compared: Control, ACM alone, ACM containing 0.5 μg BMP-9 (L-BMP-9), and ACM containing 2.0 μg BMP-9 (H-BMP-9). *$P < 0.05$ and **$P < 0.01$.

significant increases in BMD of NFB compared with baseline by week 2 in all groups. Similar to NBV, the highest increase in BMD of NFB among the groups occurred within the first 2 weeks after surgery (Table 2). The H-BMP-9 group increased rapidly between weeks 4 and 6, leading to statistically significant differences compared to the baseline values ($p < 0.01$). At 6 weeks, the new bone area fraction for the ACM/BMP-9 groups significantly increased compared to the control and RCM groups ($P < 0.05$, and $P < 0.01$, respectively). Moreover, the H-BMP-9 group had the highest amount of new bone area fraction (75.33% ± 3.78%), which was approximately 2.5-fold higher than that in the ACM group (30.35% ± 3.22%) ($P < 0.01$). Moreover, the ACM/BMP-9 groups had significantly higher new bone area fractions than that the control group ($P < 0.01$). Furthermore, the ratio in the H-BMP-9 group was markedly higher than that in the L-BMP-9 group at 4 and 6 weeks ($P < 0.05$; Fig. 3B and Table 1).

Histological findings

Histological evaluations of the experimental groups were performed to assess the osteogenic status of the regenerated tissue within the defect sites. No adverse tissue reactions were observed. In the ACM/BMP-9 groups, mature new bone was integrated with the host bone at the marginal aspect of the defect. Notably, in the images of H-BMP-9, mature new bone developed, and bone marrow cavity-like morphology was observed in the marginal aspect of the defects. The mature new bone was significantly higher in the ACM/BMP-9 groups than in the ACM and control groups. Furthermore, in the BMP-9 treated groups, osteoblasts, osteocytes and blood vessels were found within the NFB (Fig. 5).

Discussion

The primary objective of this investigation was to examine the impact of ACM and BMP-9 combined on bone formation within rat mandibular bone defects. The study hypothesized that the application of ACM/BMP-9 would facilitate the regeneration of bone tissue in standardized mandibular defects of rats. Notably, this study is pioneering in its approach by conducting real-time in vivo micro-CT analysis to evaluate the efficacy of ACM/BMP-9, ACM alone, and a

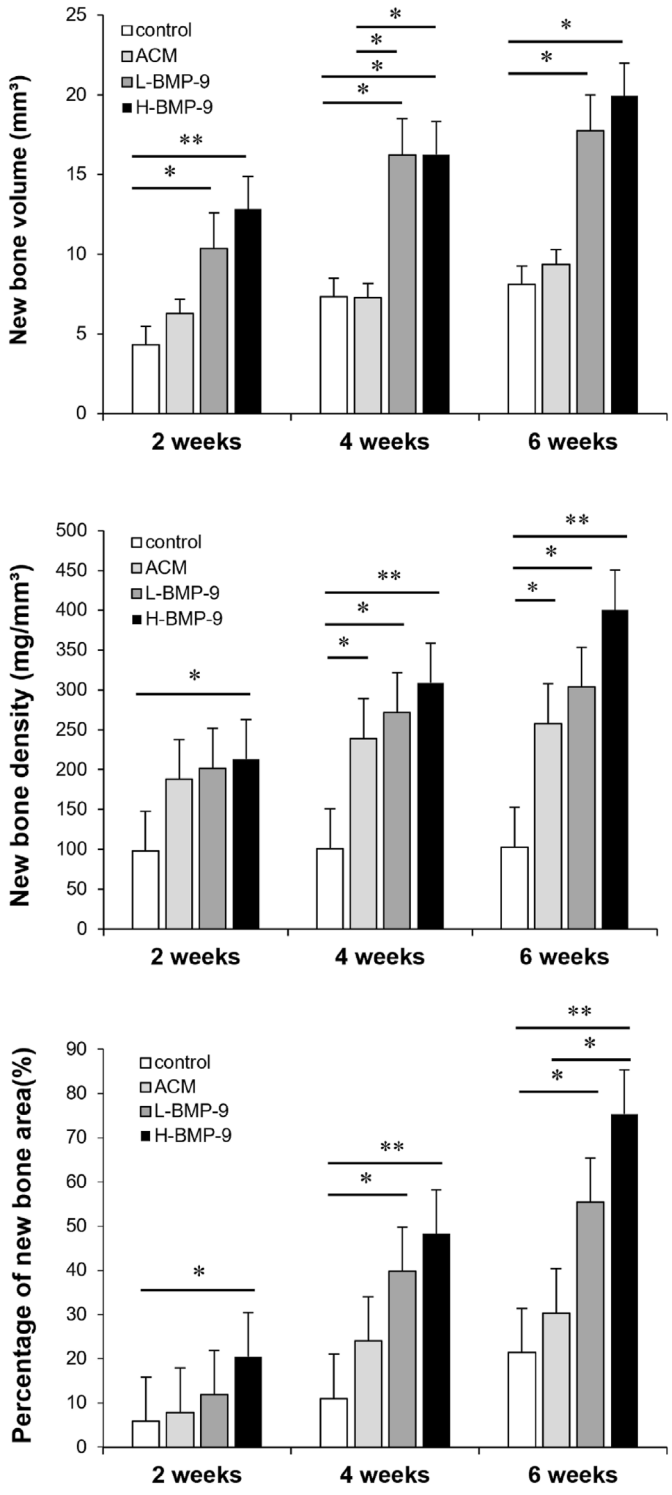

Figure 4 This figure summarizing each group by observation period. The quantitative micro-CT analysis of new bone formation, (a) bone volume (mm^3), (b) new bone density (mg/cm^3), and (c) the percentage of new bone area (%) in rat mandible defects treated with absorbable collagen membrane (ACM)/bone morphogenetic protein (BMP)-9 throughout the experimental period. Four groups were compared: Control, ACM alone, ACM containing 0.5 μg BMP-9 (L-BMP-9), and ACM containing 2.0 μg BMP-9 (H-BMP-9). *$P < 0.05$ and **$P < 0.01$.

control group in GBR surrounding mandibular osseous defects at 6 weeks post-surgery.

In our current research, we established that the ACM/BMP-9 group exhibited a substantial increase in new bone formation, demonstrating greater efficacy in closing bone defects and expanding the area of newly formed bone, in comparison to both the control group and the ACM alone group. Additionally, the H-BMP-9 group displayed the most

Table 1 Volume, mineral density, and percentage of area parameters for newly formed bone in four groups at different data collection periods.

Test groups (n = 5 per group)	Data collection period (weeks)	Newly formed bone [mean (SD)]		
		Volume (mm^3)	Mineral density (mg/mm^3)	Area (%)
control	0	—	—	—
	2	**4.31** (0.81)	**97.91** (0.95)	**5.88** (1.42)
	4	**7.35** (0.77)[c]	**100.77** (0.98)	**11.01** (1.51)
	6	**8.10** (1.55)[c]	**102.53** (1.08)	**21.35** (1.88)[c]
RCM	0	—	—	—
	2	**6.27** (1.22)	**187.91** (8.32)[a]	**7.88** (1.21)
	4	**7.26** (0.99)	**238.77** (8.57)[a,c]	**24.01** (2.47)
	6	**9.37** (2.01)[c]	**257.53** (8.79)[a,c,e]	**30.35** (3.22)[c]
L-BMP-9	0	—	—	—
	2	**10.36** (1.88)[a]	**201.91** (11.66)[a]	**11.84** (2.43)[a]
	4	**16.25** (3.19)[a,c]	**271.77** (42.95)[a,c]	**39.79** (2.78)[b]
	6	**17.75** (5.34)[a,d]	**303.53** (96.53)[a,d]	**55.46** (3.14)[b,d,f]
H-BMP-9	0	—	—	—
	2	**12.83** (5.20)[a]	**212.91** (60.9)[a]	**20.44** (1.88)[a]
	4	**16.26** (3.89)[a,c]	**308.77** (65.68)[b,d]	**48.29** (2.74)[b]
	6	**19.93** (2.66)[b,d]	**400.53** (62.49)[b,d,f]	**75.33** (3.78)[b,d,f]

ACM = Absorbable collagen membrane; L-BMP-9 = ACM containing 0.5 μg of bone morphogenetic protein-9 (BMP-9); H-BMP-9 = ACM containing 2.0 μg of BMP-9; SD = Standard deviation.

[a] Statistically significant increase compared with baseline ($P < 0.05$).
[b] Statistically significant increase compared with baseline ($P < 0.01$).
[c] Statistically significant increase compared with 2 weeks ($P < 0.05$).
[d] Statistically significant increase compared with 2 weeks ($P < 0.01$).
[e] Statistically significant increase compared with 4 weeks ($P < 0.05$).
[f] Statistically significant increase compared with 4 weeks ($P < 0.01$).

Table 2 Mean rates of change in volume, mineral density, and the percentage of area parameters for newly formed bone in four groups at different data collection periods.

Test groups (n = 5 per group)	Data collection period (weeks)	Newly formed bone		
		Rate of increase in volume (mm^3/week)	Rate of increase in mineral density (mg/mm^3/week)	Percentage of area (%/week)
control	0–2	**4.31**	**97.91**	**5.88**
	2–4	**3.04**	**2.86**	**5.13**
	4–6	**0.75**	**1.76**	**10.34**
RCM	0–2	**6.27**	**187.91**	**7.88**
	2–4	**1.99**	**50.86**	**16.13**
	4–6	**2.11**	**18.76**	**6.34**
L-BMP-9	0–2	**10.36**	**201.91**	**11.84**
	2–4	**5.89**	**69.86**	**27.95**
	4–6	**1.50**	**31.76**	**15.67**
H-BMP-9	0–2	**12.83**	**212.91**	**20.44**
	2–4	**3.43**	**95.86**	**27.85**
	4–6	**3.67**	**91.76**	**27.04**

ACM = Absorbable collagen membrane; L-BMP-9 = ACM containing 0.5 μg of bone morphogenetic protein-9 (BMP-9); H-BMP-9 = ACM containing 2.0 μg of BMP-9; SD = Standard deviation.

significant closure of defects among all experimental groups. These findings partially corroborate earlier studies indicating that the use of rhBMP-2 with a collagen membrane expedited bone formation in rat calvaria defect models.[23]

However, an increasing number of recent studies have suggested that the clinical application of rhBMP-2 for bone regeneration can lead to adverse effects such as tissue inflammation/swelling[24,25] and bone resorption[26] in human subjects. Consequently, there is a growing demand for the

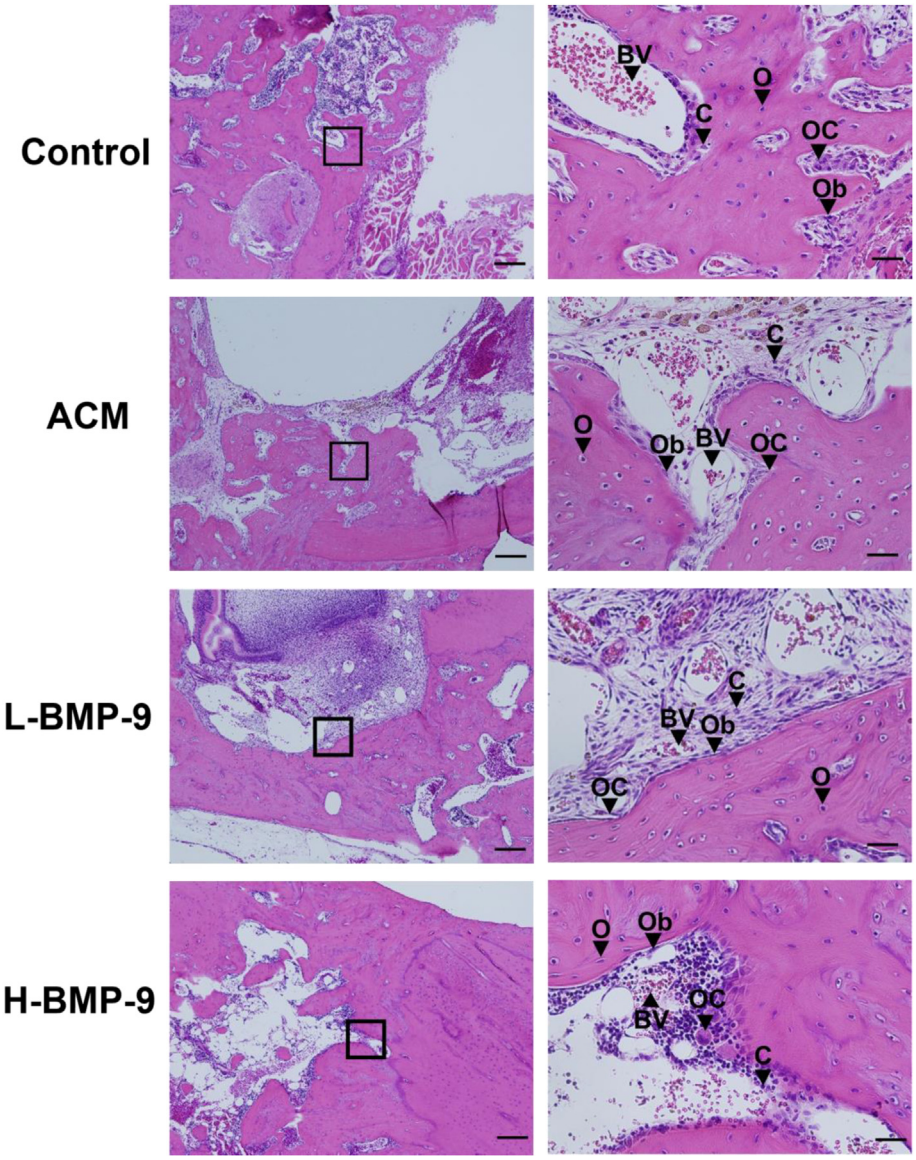

Figure 5 Light microscopic images (×4—40) show regenerated bone at 6 weeks after applying of absorbable collagen membrane (ACM)/bone morphogenetic protein (BMP)-9 at rat mandibular bone defects. NFB at the periphery of a mandibular defect was observed in BMP-9 treated groups. In addition, in the ACM containing 2.0 μg BMP-9 (H-BMP-9) group, mature lamella bone was seen and the defect tended to coalesce with the NFB. ACM containing 0.5 μg BMP-9 (L-BMP-9) group showed similar effects with the newly formed mature bone. The specimens were stained with hematoxylin and eosin (HE). Scale burs indicate 100 μm and 50 μm in low- and high-magnification images, respectively. HB: host bone, NB: Newly formed bone, F: fibrous tissue, Ob: Osteoblast, O: Osteocyte, BV: Blood vessel. Representative histological sections of ACM/BMP-9 treatment groups at high magnification (40×) showing NB, Ob, O, and BV.

development of bone regenerative therapies that are more predictable, efficient, and safe, with minimal to no complications. In recent times, there has been a growing interest in utilizing rhBMP-9 as a potential growth factor for bone regeneration, primarily because it exhibits unique properties distinct from rhBMP-2. Studies suggest that rhBMP-9 could be employed effectively at reduced doses compared to other BMPs.[27—30]

Research indicates that BMP-9 plays a crucial role in various physiological functions, such as neuronal development,[31] adipocyte differentiation,[32] chondrogenesis,[33] regulation of glucose levels,[34] and promotion of angiogenesis.[35]

Furthermore, it is currently recognized that BMP-9 activates new bone formation through a different mechanism compared to BMP-2 and exhibits complete resistance to noggin, a well-known BMP antagonist.[28—30] In terms of its osteoinductive properties, several studies utilizing adenoviruses expressing BMP-9 have shown its potential to stimulate substantial and mature ectopic bone formation.[36—38] Additionally, earlier findings suggest that combining collagen membranes with rhBMP-9 notably enhances

osteogenic differentiation of ST2 stromal bone marrow cells compared to rhBMP-2.[39] In the previous study, it was revealed that BMP-2 or BMP-7 combined with heparinized collagen membrane significantly induced new bone formation in rat calvarial defects.[40] BMP-2-releasing collagen membranes promote osteogenesis as demonstrated through osteoblast differentiation in vitro and facilitate new bone formation at 4 weeks in a mouse model.[41] However, there are currently no studies comparing a novel device incorporating BMP-9 and other BMPs as a career in ACM under the same conditions. The future research on this topic will further establish evidence of the effectiveness of BMP-9. Our findings demonstrate that BMP-9 exhibited osteoinductive properties when combined with ACM, which served as an effective vehicle for sustained delivery. Analysis using micro-CT revealed uniform distribution of new bone formation within the standardized mandibular defects as early as two weeks in the ACM/BMP-9 groups, whereas such formation was limited to the peripheries of the circular bone defects in the control and ACM groups. Additionally, our study unveiled a progressive increase in new bone formation, BMD, and percentage of new bone area within the standardized mandibular defects in the ACM/BMP-9 groups. These improvements in bone regeneration were observed in the BMP-9-treated groups with increasing concentrations of BMP-9. Real-time micro-CT images depicted radiopaque areas in the L-BMP-9 group with less bone formation within the defects compared to the H-BMP-9 group. Similar volumes of new bone formation were noted between the two groups at two weeks, followed by a rapid increase until six weeks in the H-BMP-9 group. Moreover, there were similarities in BMD between the L-BMP-9 and H-BMP-9 groups. Furthermore, the ACM/BMP-9-treated groups exhibited significantly enhanced bone regeneration within the mandibular defects compared to the control and ACM groups. These findings suggest that ACM/BMP-9 promotes new bone formation in rat mandibular defects during the early postoperative phase.

The groups with ACM implants exhibited higher levels of new bone formation compared to the control group at both 4 and 6 weeks. These results suggest that the ACM utilized in this study effectively maintained the space within the surgically created bone defects, preventing their collapse. Moreover, the slow-biodegradation properties of the ACM, which was a cross-linked collagen carrier, provided an additional advantage by preventing rapid material degradation. Prior research by Rothamel et al. demonstrated that the biodegradation of cross-linked collagen membranes is notably slower when compared to non-cross-linked membranes.[42] Additionally, Shiozaki et al. reported the presence of remnants of collagen sponge at 4 weeks post-surgery in their rat calvarial study investigating rhBMP-4 with the same cross-linked collagen sponge.[43] Our previously reported in vitro results investigating the cytotoxicity of ACM indicated that since ACM did not affect cell viability, it is considered to be a biocompatible material.[16,17] Furthermore, in this study, bone closure in the BMP-9-treated groups reached the desired volume, surpassing both the ACM alone and control groups. This suggests that ACM did not interfere with the osteoinductive potential of the combined device. Notably, there were no indications of a foreign body reaction detected throughout the in vivo study. These findings, in conjunction with our results, indicate that rhBMP-9 has the capability to adsorb ACM and that ACM serves as a carrier for BMP protein. Further investigations examining the binding and releasing kinetics of BMP-9 are essential to gain a better understanding of the delivery mechanisms of ACM. Additionally, in vitro and in vivo studies utilizing different carrier systems and observation periods are required to clarify these inquiries.

Recent reports have highlighted the potential for high doses of rhBMP-2 in clinical use to lead to various adverse effects such as tissue inflammation/swelling[25,44] and bone resorption.[26] Consequently, there is a pressing need for the development of bone regenerative therapies that are more predictable, effective, and safe. A comparative study evaluating the application of BMP-2, -4, and -7 (each at 2.5 μg/site) in rat calvarial defects found no significant differences in their bone regenerative potential. In our current study, ACM combined with either 0.5 or 2.0 mg/site of rhBMP-9 significantly accelerated new bone formation compared to ACM alone. Gaihre et al. showed that the chitosan microparticles coated with rhBMP-9 (0.5 μg or 1.5 μg) could enhance newly formed bone in a critical-sized rat cranial defect at 8 weeks after surgery.[45] BMP-9 (2.5 μg) with absorbable collagen sponge (BMP-9/ACS) was tested in vivo to determine the biological response in a rat calvarial critical-size defect at 2 and 8 weeks. The BMP-9/ACS groups significantly induced new bone formation compared to the control and ACS alone groups at 8 weeks post-surgery.[20] Another study showed that rhBMP-9 (1.0 μg)/ACS has a potential to induce bone formation in rat calvarial bone defects at 8 weeks.[46] In our present experiment, 0.5 μg or 2.0 μg of rhBMP-9 was applied and considered to be adequate. This suggests that even at lower doses, rhBMP-9 exhibits potent osteoinductive activity. It is speculated that the mechanisms underlying BMP-9-mediated osteoinduction differ from those of other BMPs.[47] For instance, Leblanc et al. demonstrated that BMP-9 induces heterotrophic ossification only in damaged skeletal muscle, whereas BMP-2 can induce it in both damaged and undamaged muscle.[27] Moreover, BMP-9 possesses unique characteristics such as a non-inhibitory effect on bone formation[36] and resistance to noggin inhibition.[28–30] These findings suggest the possibility of using reduced dosages of rhBMP-9 to minimize future clinical complications and that the clinical outcomes of rhBMP-9 may differ from those of other BMPs in bone healing/regenerative therapy. Further investigation is warranted to elucidate the bone healing/regenerative potential of rhBMP-9 compared to other BMPs, particularly rhBMP-2, under similar in vivo conditions (such as species and age of animals, defect size, carrier/scaffold, and observation period). The accumulating evidence regarding BMP-9 may open up a wide range of possibilities for utilizing rhBMP-9 in bone healing/regenerative procedures in both dental and medical fields.

Within the constraints of this study, we propose that ACM/BMP-9 could be effective in stimulating bone regeneration in critical size mandibular defects in rats. Further investigations are warranted to confirm the effects of BMP-9 on bone regeneration in larger animal models, with potential implications for clinical use in humans.

This study demonstrates significantly improved qualitative and quantitative bone regeneration in standardized rat

mandibular bone defects using a novel combination of ACM/BMP-9. The inclusion of BMP-9 notably boosted bone formation six weeks after application, leading to enhanced bone regeneration and complete closure of defects when incorporated at an appropriate concentration within ACMs. These findings underscore the clinical relevance of this study, spanning applications from osseous defect regeneration to ridge augmentation and dental implantation, ensuring sufficient alveolar bone quantity.

Declaration of competing interest

The authors have no conflicts of interest relevant to this article.

Acknowledgments

We thank the Department of Oral Health Sciences, Nihon University School of Dentistry, for technical advice and assistance, and the Department of Pathology, Nihon University School of Dentistry, for histological imaging. We also thank Prof. Yoshinori Arai who assisted and commented on the micro-CT analysis. We thank the Ito Bone Histomorphometry Institute for analyzing histological sections of newly formed bone.

This research was supported in part by a Grant-in-Aid for Scientific Research (C) (No. JP22K09973 to T. Takayama) from the Ministry of Education, Culture, Sports, Science and Technology of Japan, Grant from Dental Research Center, Nihon University School of Dentistry (to T. Takayama), and the Sato Fund, Nihon University School of Dentistry (to T. Takayama).

References

1. Rocchietta I, Fontana F, Simion M. Clinical outcomes of vertical bone augmentation to enable dental implant placement: a systematic review. *J Clin Periodontol* 2008;35:203—15.
2. Elgali I, Omar O, Dahlin C, Thomsen P. Guided bone regeneration: materials and biological mechanisms revisited. *Eur J Oral Sci* 2017;125:315—37.
3. Miron RJ, Zhang Q, Sculean A, et al. Osteoinductive potential of 4 commonly employed bone grafts. *Clin Oral Invest* 2016;20:2259—65.
4. Abtahi S, Chen X, Shahabi S, Nasiri N. Resorbable membranes for guided bone regeneration: critical features, potentials, and limitations. *ACS Mater Au* 2023;3:394—417.
5. Cucchi A, Chierico A, Fontana F, et al. Statements and recommendations for guided bone regeneration: consensus report of the guided bone regeneration symposium held in Bologna, October 15 to 16, 2016. *Implant Dent* 2019;28:388—99.
6. Sasaki J, Abe GL, Li A, et al. Barrier membranes for tissue regeneration in dentistry. *Biomater Investig Dent* 2021;8:54—63.
7. Ferreira AM, Gentile P, Chiono V, Ciardelli G. Collagen for bone tissue regeneration. *Acta Biomater* 2012;8:3191—200.
8. Wang HL, Carroll WJ. Guided bone regeneration using bone grafts and collagen membranes. *Quintessence Int* 2001;32:504—15.
9. Urban IA, Wessing B, Alandez N, et al. A multicenter randomized controlled trial using a novel collagen membrane for guided bone regeneration at dehisced single implant sites: outcome at prosthetic delivery and at 1-year follow-up. *Clin Oral Implants Res* 2019;30:487—97.
10. Khorsand B, Elangovan S, Hong L, Kormann MSD, Salem AK. A bioactive collagen membrane that enhances bone regeneration. *J Biomed Mater Res B Appl Biomater* 2019;107:1824—32.
11. Sam G, Pillai BRM. Evolution of barrier membranes in periodontal regeneration-"Are the third generation membranes really here?". *J Clin Diagn Res* 2014;8:ZE14—7.
12. Bee SL, Hamid ZAA. Asymmetric resorbable-based dental barrier membrane for periodontal guided tissue regeneration and guided bone regeneration: a review. *J Biomed Mater Res B Appl Biomater* 2022;110:2157—82.
13. Mitchell AC, Briquez PS, Hubbell JA, Cochran JR. Engineering growth factors for regenerative medicine applications. *Acta Biomater* 2016;30:1—12.
14. Koons GL, Mikos AG. Progress in three-dimensional printing with growth factors. *J Contr Release* 2019;295:50—9.
15. Yamano S, Haku K, Yamanaka T, et al. The effect of a bioactive collagen membrane releasing PDGF or GDF-5 on bone regeneration. *Biomaterials* 2014;35:2446—53.
16. Takayama T, Dai J, Tachi K, et al. The potential of stromal cell-derived factor-1 delivery using a collagen membrane for bone regeneration. *J Biomater Appl* 2017;31:1049—61.
17. Ozaki M, Takayama T, Yamamoto T, et al. A collagen membrane containing osteogenic protein-1 facilitates bone regeneration in a rat mandibular bone defect. *Arch Oral Biol* 2017;84:19—28.
18. Furuhata M, Takayama T, Yamamoto T, et al. Real-time assessment of guided bone regeneration in critical size mandibular bone defects in rats using collagen membranes with adjunct fibroblast growth factor-2. *J Dent Sci* 2021;16:1170—81.
19. Sreekumar V, Aspera-Werz RH, Tendulkar G, et al. BMP9 a possible alternative drug for the recently withdrawn BMP7? New perspectives for (re-)implementation by personalized medicine. *Int J Arch Toxicol* 2017;91:1353—66.
20. Nakamura T, Shirakata Y, Shinohara Y, et al. Comparison of the effects of recombinant human bone morphogenetic protein-2 and -9 on bone formation in rat calvarial critical-size defects. *Clin Oral Invest* 2017;21:2671—9.
21. Fujioka-Kobayashi M, Raouf MAE, Saulacic N, et al. Superior bone-inducing potential of rhBMP9 compared to rhBMP2. *J Biomed Mater Res A* 2018;106:1561—74.
22. Stewart SK. Fracture Non-Union: a review of clinical challenges and future research needs. *Malays Orthop J* 2019;13:1—10.
23. Pelaez M, Susin C, Lee J, et al. Effect of rhBMP-2 dose on bone formation/maturation in a rat critical-size calvarial defect model. *J Clin Periodontol* 2014;41:827—36.
24. Tumialán LM, Rodts GE. Adverse swelling associated with use of rh-BMP-2 in anterior cervical discectomy and fusion. *Spine J* 2007;7:509—10.
25. Smucker JD, Rhee JM, Singh K, Yoon ST, Heller JG. Increased swelling complications associated with off-label usage of rhBMP-2 in the anterior cervical spine. *Spine (Phila Pa 1976)* 2006;31:2813—9.
26. McClellan JW, Mulconrey DS, Forbes RJ, Fullmer N. Vertebral bone resorption after transforaminal lumbar interbody fusion with bone morphogenetic protein (rhBMP-2). *J Spinal Disord Tech* 2006;19:483—6.
27. Leblanc E, Trensz F, Haroun S, et al. BMP-9-induced muscle heterotopic ossification requires changes to the skeletal muscle microenvironment. *J Bone Miner Res* 2011;26:1166—77.
28. Rosen V. BMP and BMP inhibitors in bone. *Ann N Y Acad Sci* 2006;1068:19—25.
29. Nakamura T, Shinohara Y, Momozaki S, Yoshimoto T, Noguchi K. Co-stimulation with bone morphogenetic protein-9 and FK506 induces remarkable osteoblastic differentiation in rat dedifferentiated fat cells. *Biochem Biophys Res Commun* 2013;440:289—94.

30. Wang Y, Hong S, Li M, et al. Noggin resistance contributes to the potent osteogenic capability of BMP9 in mesenchymal stem cells. *J Orthop Res* 2013;31:1796—803.
31. López-Coviella I, Berse B, Krauss R, Thies RS, Blusztajn JK. Induction and maintenance of the neuronal cholinergic phenotype in the central nervous system by BMP-9. *Science* 2000;289:313—6.
32. Lord E, Bergeron E, Senta H, Park H, Faucheux N. Effect of BMP-9 and its derived peptide on the differentiation of human white preadipocytes. *Growth Factors* 2010;28:149—56.
33. Majumdar MK, Wang E, Morris EA. BMP-2 and BMP-9 promotes chondrogenic differentiation of human multipotential mesenchymal cells and overcomes the inhibitory effect of IL-1. *J Cell Physiol* 2001;189:275—84.
34. Chen C, Grzegorzewski KJ, Barash S, et al. An integrated functional genomics screening program reveals a role for BMP-9 in glucose homeostasis. *Nat Biotechnol* 2003;21:294—301.
35. Ricard N, Ciais D, Levet S, et al. BMP9 and BMP10 are critical for postnatal retinal vascular remodeling. *Blood* 2012;119:6162—71.
36. Kang Q, Sun MH, Cheng H, et al. Characterization of the distinct orthotopic bone-forming activity of 14 BMPs using recombinant adenovirus-mediated gene delivery. *Gene Ther* 2004;11:1312—20.
37. Luu HH, Song WX, Luo X, et al. Distinct roles of bone morphogenetic proteins in osteogenic differentiation of mesenchymal stem cells. *J Orthop Res* 2007;25:665—77.
38. Li JZ, Li H, Sasaki T, et al. Osteogenic potential of five different recombinant human bone morphogenetic protein adenoviral vectors in the rat. *Gene Ther* 2003;10:1735—43.
39. Fujioka-Kobayashi M, Sawada K, Kobayashi E, Schaller B, Zhang Y, Miron RJ. Recombinant human bone morphogenetic protein 9 (rhBMP9) induced osteoblastic behavior on a collagen membrane compared with rhBMP2. *J Periodontol* 2016;87:101—7.
40. Jo JY, Jeong SI, Shin YM, et al. Sequential delivery of BMP-2 and BMP-7 for bone regeneration using a heparinized collagen membrane. *Int J Oral Maxillofac Surg* 2015;44:921—8.
41. Chung EJ, Chien KB, Aguado BA, Shah RN. Osteogenic potential of BMP-2-releasing self-assembled membranes. *Tissue Eng Part A* 2013;19:2664—73.
42. Rothamel D, Schwarz F, Sager M, Herten M, Sculean A, Becker J. Biodegradation of differently cross-linked collagen membranes: an experimental study in the rat. *Clin Oral Implants Res* 2005;16:369—78.
43. Shiozaki Y, Kitajima T, Mazaki T, et al. Enhanced in vivo osteogenesis by nanocarrier-fused bone morphogenetic protein-4. *Int J Nanomed* 2013;8:1349—60.
44. Tumialán LM, Rodts GE. Adverse swelling associated with use of rh-BMP-2 in anterior cervical discectomy and fusion. *Spine J* 2007;7:509—10.
45. Gaihre B, Bharadwaz A, Unagolla JM, Jayasuriya AC. Evaluation of the optimal dosage of BMP-9 through the comparison of bone regeneration induced by BMP-9 versus BMP-2 using an injectable microparticle embedded thermosensitive polymeric carrier in a rat cranial defect model. *Mater Sci Eng C Mater Biol Appl* 2021;127:112252.
46. Shinohara Y, Nakamura T, Shirakata Y, Noguchi K. Bone healing capabilities of recombinant human bone morphogenetic protein-9 (rhBMP-9) with a chitosan or collagen carrier in rat calvarial defects. *Dent Mater J* 2016;35:454—60.
47. Lamplot JD, Qin J, Nan G, et al. BMP9 signaling in stem cell differentiation and osteogenesis. *Am J Stem Cells* 2013;2:1—21.